Analysis of Low-Concentration Solar Photovoltaic Systems: A Comparative Study of Concentrator Geometries

Ikaro T. B. S. Barreto [1], Leonardo F. L. de Souza [2], Chigueru Tiba [1], José L. A. Da Silva [2] and Felipe M. Nogueira [2]

[1] Universidade Federal de Pernambuco, Recife, (Brasil)

[2] Universidade Federal de Alagoas, Rio Largo, (Brasil)

Abstract

The demand for sustainable energy solutions has led to the development of low-concentration photovoltaic (LCPV) systems to improve solar energy conversion efficiency. This study investigates a solar concentrator model, evaluating its efficiency and irradiance uniformity on the receiver. Computational modeling and performance analysis were conducted using SolTrace software, with precise system modeling. The study analyzed three configurations: a Linear Fresnel concentrator adapted which combines Compound Parabolic Concentrator (CPC) irradiance uniformity with Fresnel tracking flexibility; a V-Trough and a truncated CPC models based on previous studies. The comparative analysis evaluated parameters such as irradiance uniformity, acceptance angle, intercept factors and concentration efficiency under varying conditions. The results contribute to optimizing LCPV systems, improving energy efficiency.

Keywords: Low-Concentration Photovoltaic Systems, SolTrace, Fresnel Concentrator, CPC, V-Trough, Energy Efficiency.

1. Introduction

Various technologies are currently employed to generate energy using solar radiation. The main Photovoltaic (PV), which basically consists of the conversion of photons (sunlight) into electricity, has shown a reduction in its cost and has become increasingly established in recent years. Furthermore, this energy source contributes significantly to the reduction of greenhouse gas emissions, assisting and continuing to assist the global energy transition toward a renewable matrix in the coming years (GARLET et al., 2022).

Geometrical optics applied to solar generation allows for the concentration of insolation onto point or linear foci. Energy generation technologies through solar concentration have seen progress in research and technological advancements in recent years to enable their application for commercial purposes. They can become one of the keys to expanding the global electricity sector, especially in the current moment where the energy transition toward more sustainable production and consumption systems is widely discussed. It has enabled the development of energy utilization devices that have been applied to desalination, thermoelectric generation, chemical reactors, heat generation for industrial processes, among others (SOUZA, 2022).

The efficiency of PV modules has been increasing while production and installation costs have decreased, thanks to studies on applied materials, cell construction, and manufacturing techniques. Beyond the conventional use of PV modules, there is the possibility of solar energy production through the use of solar concentration devices integrated with photovoltaic modules, establishing Concentration Photovoltaic (CPV) systems. In operation, CPV concentrates sunlight onto the cells using lenses or mirrors. This allows for higher energy generation per surface area, as it increases the intensity of solar radiation incident on the target surface.

In this scenario, the LCPV systems emerge as a viable alternative by using optical elements to concentrate sunlight onto PV cells with relatively low concentration ratios, typically between 1.5x and 10x (Kolamroudi et al., 2023). These systems offer attractive advantages concerning a higher power density. This, consequently,

10.18086/swc.2025.03.03 Available at http://proceedings.ises.org

can provide a reduction in the costs of the system as a whole. However, the objective of this work is not to discuss the economic advantages and commercialization potential of this technology, but rather to present studies focused on the comparison of concentrator models applicable in LCPV and to seek advances in their optimization, and also analyse the critical challenge in these systems that lies in ensuring irradiance uniformity on the PV receiver to avoid localized heating and efficiency drops.

Based on established solar concentration technologies, this study investigates and adapts several promising designs, validating their quality in comparison to other models based on parameters such as solar ray uniformity, interception factor, and acceptance angle. The initial endeavor involves the configuration of a V-Trough model, which has a simpler design. Its fundamental principles are extracted from the research conducted by Parupudi et al. (2020), with a complementary analysis of its operational characteristics informed by the earlier work of Fraidenraich and Almeida (1991).

In parallel, a Truncated CPC (Compound Parabolic Concentrator) model was analyzed, previously obtained through the study by Xie et al. (2016), particularly the development of a CPC model with a reduced truncation point, known as Higher Effective Multiple Reflections (HEMR). Considering these diverse yet related approaches, this investigation aims to explore and potentially optimize solar concentration strategies for improved performance and practicality.

Finally, the linear Fresnel model is conceived through a derivation process based on a CPC developed by the authors but which presented some limitations in its acceptance angle. The central premise is to leverage the well-documented uniformity of solar flux distribution inherent in CPC designs and incorporate this advantage into a Fresnel reflector-based system following the original geometry. The proposed methodology seeks to optimize solar tracking requirements while achieving enhanced solar angle coverage.

2. Methodology

This section details the investigation process and the tools utilized to evaluate and optimize solar concentration strategies.

The study began with a bibliographic review focused on previous studies concerning LCPV, aiming to identify analysis methodologies and conversion efficiency results. Based on this analysis, three established linear solar concentration technologies were selected and adapted:

2.1.1 V-Trough:

The initial model was configured based on the fundamental principles of research by Parupudi et al. (2020), complemented by an analysis of the operational characteristics presented by Fraidenraich and Almeida (1991).

2.1.2 Truncated CPC (Compound Parabolic Concentrator):

A truncated CPC model with a reduced truncation point (known as Lower Effective Multiple Reflections - LEMR) was analyzed, as developed by Xie et al. (2016).

2.1.3 Linear Fresnel Concentrator:

This model was conceived through a derivation process, adapting the geometry of a CPC previously developed by the authors. The central premise was to transfer the recognized uniformity of the CPC's solar flux distribution to a system based on Fresnel reflectors, while maintaining the original geometry.

2.2 Geometric Modeling and Ray Tracing Simulation:

The core of the methodology involved the modeling and simulation of the concentrators to analyze critical optical performance parameters.

2.2.1 Geometric Modeling (Python) and Optical Simulation (SolTrace):

The geometric equations defining the curves of each concentrator were identified and implemented using the Python programming language. This process resulted in the generation of point files (in .csi or .txt format) that defined the concentrators' geometries. The generated files were imported into the solar ray tracing software, SolTrace. was used to simulate the optical behavior of the concentrators, with the solar source following a

Gaussian distribution, which is considered more realistic for analysis purposes.

2.2.2 The models were evaluated based on three optical performance parameters:

The quality of the concentration is assessed through the coefficient of variation of Uniformity (U) and the ratio of minimum to maximum irradiance on the receiver (I_{min}/I_{max}), where higher values and lower U values indicate a more spatially homogeneous light distribution. The intercept factor (γ) quantifies the proportion of concentrated radiation that effectively reaches the receiver, with values approaching unity being desirable for maximizing energy capture. The ratio of the incidence angle (ϕ) to this characteristic maximum acceptance angle (ϕ/ϕ_{max}), a dimensionless parameter ranging from 0 to 1, serves to represent the relative angular position of the sun with respect to the collector's operational range. Values closer to 0 (normal incidence) yield optimal performance and maximum intercept factor. As ϕ/ϕ_{max} increases, indicating greater angular deviation, concentration efficiency and the intercept factor progressively decrease. Near the acceptance limit, significant energy losses occur due to reduced reflection towards the receiver. Thus, maintaining a low ϕ/ϕ_{max} is crucial for efficient solar energy collection.

2.2.3 Optimization and Parametric Analysis:

The methodology actively sought the optimization of the concentrators through adjustments to the geometric equations and variation of the concentration value (C). The behavior of the performance parameters was meticulously verified with these variations. To validate the Acceptance Angle, an adjustment was made to the SolTrace script to vary the solar angle, confirming that the Intercept Factor behaved as expected (drastic reduction upon exceeding the Acceptance Angle, θ_a).

3. CPV Review

The operating principle of the technology is to focus the DNI (Direct Normal Irradiance) onto the focal point of a reflective surface concentrator and direct it to a receiver component (Hasan et al., 2024, Kalogirou, 2009). Regarding optical concentrators, such as parabolic troughs and Fresnel lenses, these have been the subject of experiments in CPV systems (Dhakal et al., 2014, Chemisana et al., 2009, Indira et al., 2021). Depending on the level of concentration achieved, these systems can be classified as low concentration (up to 10), medium concentration (between 10 and 100), and high concentration (between 100 and 2000). Each concentration range is suitable for a specific type of solar cell (Kolamroudi et al., 2023).

Problems related to CPV power generation include increased temperature and non-uniformity of the incident irradiance on the module. Cuevas and Lopez-Romero (1984) conducted experiments indicating that the open-circuit voltage of the photovoltaic cell under non-uniform illumination is lower than under uniform illumination distribution, as in the former situation there is a reduction in the photovoltaic cell's open-circuit voltage since it would exhibit a series resistive behavior, which ultimately decreases the photovoltaic cell's efficiency (Regany et al., 2025).

The model adopted by Parupudi et al. (2020) is presented, explaining its operation, development, main results, and the fundamental properties analyzed. The study analyzed the V-Trough, along with other geometries such as the CPC and the ACPC. The primary objective is to evaluate the benefits of these configurations in improving energy efficiency in buildings by optimally harnessing solar radiation. The results indicated that the developed LCPVs exhibited electrical conversion efficiencies ranging between 15% and 17,62%, depending on the type of solar cell used (m-Si and p-Si) and the concentrator configuration. The data were processed and compared with traditional flat-plate solar modules to validate the model's efficacy.

As discussed by Xie et al. (2016), the HEMR model exhibits approximately 2% higher uniformity compared to the LEMR, which makes it more suitable for applications where optimizing the homogeneity of concentrated radiation is desired. This factor was determinant for adopting the HEMR in the present study, given that irradiance uniformity is directly associated with the performance of the coupled photovoltaic system. In addition to uniformity, another advantage relates to the acceptance angle. While the LEMR has a value of approximately 6,7°, the HEMR reaches 10,6°, which provides greater tolerance to variations in the solar incidence angle. On the other hand, a limitation of the HEMR is its geometric height, at 0,7032 m, compared to 0,5434 m for the LEMR. The lower height may offer advantages from a constructive standpoint, such as cost reduction and easier installation. However, both models demand high manufacturing precision to ensure optimal alignment and optical performance.

To organize the comparative analysis of some articles that studied CPV or LCPV technology and some of their results, Table 1 is presented.

Table 1: Table captions (8 pt) should be centered and placed above the table.

Authors	Methodology	Conclusions
Wang et al. (2020)	The CPV system using a linear Fresnel reflector (LFR) with mirrors was proposed to maximize the performance of the photovoltaic (PV) panel. The concentration was simulated using the Monte Carlo ray tracing method.	The results of their study show that the geometric concentration ratio CR and the land utilization rate increase when the height of the solar panel is raised. Furthermore, the energy conversion efficiencies for the solar cell monomer and the module were determined to be 14,7% and 13,3%, respectively.
Lofti et al. (2022)	The power output of the PV module was enhanced in an experimental system featuring two mirrors (upper and lower). As this led to an increase in module temperature, a phase-change material (PCM) was included for cooling purposes.	They concluded that the integration of the reflectors and the PCM improved the photovoltaic module's power output by 12,5% compared to the conventional PV module.
Kolamroudi et al. (2023)	The energy generated by a system with four planar mirrors, which concentrate the radiation onto a photovoltaic module, was analyzed. The system also utilized cooling. In some stages, one of the mirrors remained uncovered, while the others were covered, and in other stages, all mirrors were uncovered.	In the LCPV system tested with cooling and four mirrors, the no-load output power increased 2.84 times more than in the system without a concentrator, with the solar panel efficiency values reaching 42.68% and 15.03%, respectively.
Ustaoglu et al. (2023)	A comparison of performance among CPC, V-trough, and CHC (Compound Hyperbolic Concentrator) systems was conducted, considering various levels of reflector truncation to achieve uniform illumination and improved electrical and thermal energy conversion performance.	Truncation reduces cell temperature and provides a more uniform temperature distribution. The CPC showed a decrease in thermal energy generation by 0,5% and electrical energy generation by 1,3%; Conversely, the CHC exhibited an increase in thermal energy generation by 45,5% and 21,7% and electrical energy generation by 59,8% and 32,8% when compared to the V-trough and the CPC, respectively.

To characterize the energy distribution, several statistical parameters are generated, including: the irradiance on the k-th area element (Eq. 1), the average irradiance on the receiver at each position (Eq. 2), the standard deviation (Eq. 3), and the uniformity coefficient (Eq. 4) (Prasad et al., 2017).

$$I_k = \frac{P_r * N_k}{A_{abs}} \qquad \text{(eq. 1)}$$

$$\mu = \frac{P_{corrigido} * N_{abs}}{A_{abs}} \qquad \text{(eq. 2)}$$

$$\sigma = \sqrt{\frac{1}{N_e} \sum_{k=1}^{30} \quad (I_k - \mu)^2} \qquad \text{(eq. 3)}$$

$$U = \frac{\sigma}{\mu} \qquad \text{(eq. 4)}$$

To evaluate the system's efficiency, Souza (2022) introduced the concept of the intercept factor γ, which represents the fraction of total rays that are successfully captured by the receiver.

$$\gamma = \frac{I_{capturated}}{I_{total}} \quad \text{(eq. 5)}$$

The efficiency of a Concentrator in harnessing solar energy is intrinsically linked to a suite of optical parameters that govern the concentration and distribution of solar radiation onto the receiver. Prominent among these parameters are the concentration factor (C), which influences the intensity of the concentrated radiation; the solar disk half-angle, a fundamental constant defining the angular subtense of the light source. The maximum acceptance angle (ϕ_{max}) of a solar concentrator, which defines the operational limits with respect to solar incidence angles, is determined by the specific geometry of the optical design. The integrated analysis of these parameters is crucial for the optimization of the design and performance of solar concentration systems, ensuring efficient and uniform energy conversion. Significantly, these simulations permit the initial determination of crucial performance parameters.

4. Geometry information

This topic will present the geometries that defined each of the tested concentrators.

4.1 V-Trough

The model adopted by Parupudi et al. (2020) is presented, explaining its operation, development, main results, and the fundamental properties analyzed. The study analyzed the V-Trough, along with other geometries such as the CPC and the ACPC. The primary objective is to evaluate the benefits of these configurations in improving energy efficiency in buildings by optimally harnessing solar radiation. The results indicated that the developed LCPVs exhibited electrical conversion efficiencies ranging between 15% and 17.62%, depending on the type of solar cell used (m-Si and p-Si) and the concentrator configuration. The data were processed and compared with traditional flat-plate solar modules to validate the model's efficacy.

$$H_v = \frac{W_{a-v} - W_{r-v}}{2 * tan(\theta_T)} \quad \text{(eq. 6)}$$

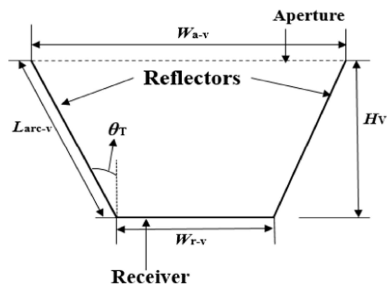

Figure 1. Model of the V-Trough concentrator.

4.2 CPC Truncado

The Truncated CPC considers fundamental optical and geometrical parameters to maximize the concentration efficiency of solar radiation onto LCPV cells. To achieve this, a non-linear system of equations was implemented, which describes the relationships between the essential geometric variables of the concentrator.

$$16(sin^2\theta + sin\theta)t_{Cl}^4 + 8(3sin^2\theta + sin\theta - 1)t_{Cl}^2 - 16sin\theta cos\theta t_{Cl} + (-3sin^2\theta + sin\theta + 2) = 0 \quad \text{(eq. 7)}$$

$$4L(sin\theta + 1)cos\theta t_{Cl}^2 + 4L(sin\theta + 1)sin\theta t_{cl} - (Lsin\theta cos\theta + Lcos\theta + 2H_l) = 0 \quad \text{(eq. 8)}$$

$$4sin\theta(sin\theta + 1)\, t_{Cl}^2 - 4cos\theta(sin\theta + 1)t_{cl} - (sin^2\theta + sin\theta - C_{LEMR} - 1) = 0 \quad \text{(eq.9)}$$

$$L(sin^2\theta + 1) - 2f_l = 0 \quad \text{(eq. 10)}$$

These equations form a coupled system that geometrically describes the behavior of solar rays reflected by the mirrors and striking the absorber. The first relates the trigonometric variables and t_{Cl}, expressing geometric constraints on the positioning of the reflected beam. The next connects the absorber width L, height H_l and the angular parameters, ensuring the absorber is positioned to capture the reflected rays. The third relates the parameter t_{Cl} to the effective concentration C, reflecting the condition that the ratio between the entrance and exit areas defines the geometric concentration. Finally, the fourth establishes the relationship between the absorber width and the parameter f_l, which influences the focal alignment.

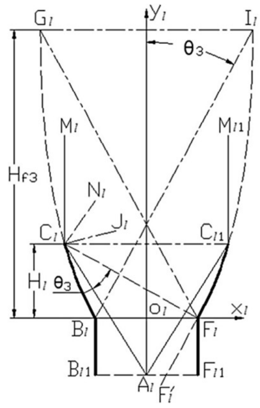

Figure 2. Model of the truncated CPC concentrator

The parametric equations for generating the System with C =4 are indicated by eq. (11) for segment CB and eq. (12) for segment C_1F. The value of t_{cl} ranges between 0,400 and 1,230.

$$\{x = 83{,}7\; t_{Cl}^2 - 371{,}3t_{cl} + 57{,}1;\;\; y = 371{,}3\; t_{Cl}^2 + 83{,}7t_{cl} - 92{,}8 \qquad \text{(eq. 11)}$$

$$\{x = -83{,}7\; t_{Cl}^2 + 371{,}3t_{cl} - 57{,}1\;;\; y = 371{,}3\; t_{Cl}^2 + 83{,}7t_{cl} - 92{,}8 \qquad \text{(eq. 12)}$$

Following the adjustments for optimization, the concentration was changed to C =3,25. With this adjustment, the acceptance angle increased to 14,03°. The concentrator height was reduced to 510,25mm. The parametric equations became Eq. (13) for segment CB and Eq. (14) for segment C_1F. The value of t_{cl} ranges between 0,39 and 1,149.

$$\{x = 94{,}0\; t_{Cl}^2 - 376{,}1t_{cl} + 54{,}5\; y = 376{,}1\; t_{Cl}^2 + 94{,}0t_{cl} - 94{,}0 \qquad \text{(eq. 13)}$$

$$\{x = -94{,}0\; t_{Cl}^2 + 376{,}1t_{cl} - 54{,}5\; y = 376{,}1\; t_{Cl}^2 + 94{,}0t_{cl} - 94{,}0 \qquad \text{(eq. 14)}$$

4.3 Fresnel derived from a CPC

The modeled collector is composed of a reflector, which consists of two identical mirrors, and a receiver (or absorber), which receives the solar radiation reflected by the reflector, as shown in Fig. 3.

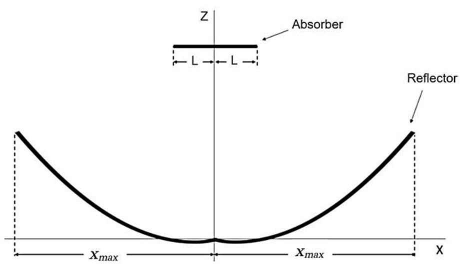

Figure 3. Geometry of the CPC.

Considering the collector with a concentration factor C and with the dimensions shown in Fig. 3, the relationship between the maximum abscissa value of the reflector and the receiver is obtained, given by Eq. (15).

$$x_{max} = CL \qquad \text{(eq. 15)}$$

The cross-section of the reflector is symmetrical with respect to the Z-axis. Therefore, the equation that defines this curve can be obtained from the modeling of only one of its halves, as shown in Fig. 4.

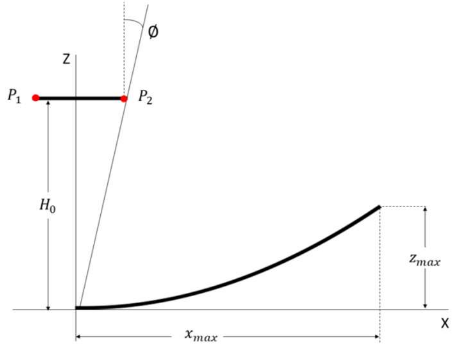

Figure 4. Geometry of half the CPC.

The modeling of the reflector consists of finding a curve that guarantees that, for ϕ qual to zero, all rays hitting the mirror are directed to the receiver with uniform irradiance. The equation that describes such a curve is obtained from Eq. (16), the equation of reflection (Burkhard and Shealy, 1975).

$$\vec{r} = \vec{I} - 2\vec{N}(\vec{N} * \vec{I}) \quad \text{(eq. 16)}$$

Where $\vec{r}$ is the unit vector of the reflected ray, $\vec{I}$ is the unit vector of the incident ray, and $\vec{N}$ is the unit vector normal to the surface at the point where the ray strikes it.

$$\vec{I} = (sen\phi, -cos\phi) \quad \text{(eq. 17)}$$

$$\vec{N} = \frac{(z',1)}{\sqrt{z'^2+1}} \quad \text{(eq. 18)}$$

Substituting Eq. (17) and Eq. (18) into Eq. (16), Eq. (19) is obtained.

$$\vec{r} = \left[\frac{sen\phi(z'^2+1)-2z'(z'sen\phi+cos\phi)}{(z'^2+1)}\right]\hat{\imath} + \left[\frac{-cos\ \ (z'^2+1)-2z'(z'sen\phi+cos\phi)}{(z'^2+1)}\right]\hat{k} \quad \text{(eq. 19)}$$

Dividing the second term on the right side of Eq. (19) by the first term on the right side of Eq. (19) results in Eq. (20).

$$\frac{r_z}{r_x} = \frac{z'^2-1-2z'tan\phi}{z'^2tan\phi-tan\phi+2z'} \quad \text{(eq. 20)}$$

Letting X be the abscissa of the point on the receiver that receives the reflected ray at a point with abscissa x on the reflector, Eq. (21) is obtained.

$$\frac{r_z}{r_x} = \frac{H_0-z}{X-x} \quad \text{(eq. 21)}$$

Substituting Eq. (21) into Eq. (20), Eq. (22) is obtained.

$$z'^2(1 - tan\phi) + z'\left[-2tan\phi - 2\left(\frac{H_0-z}{X-x}\right)\right] + \left(\frac{H_0-z}{X-x}\right) tan\phi - 1 = 0 \quad \text{(eq. 22)}$$

The solutions of Eq. (22) for the variable z' are given by Eq. (23) and Eq. (24).

$$z' = \frac{sen\phi(X-x)+cos\phi(H_0-z)-R}{cos\phi(X-x)-(H_0-z)sen\phi} \quad \text{(eq. 23)}$$

$$z' = \frac{sen\phi(X-x)+cos\phi(H_0-z)+R}{cos\phi(X-x)-(H_0-z)sen\phi} \quad \text{(eq. 24)}$$

Where R is given by Eq. (25).

$$R = \sqrt{(H_0 - z)^2 + (X - x)^2} \quad \text{(eq. 25)}$$

The sign used before the term “R” in Eq. (23) and Eq. (24) determines the concavity of the resulting curve. If the sign is positive, the curve's concavity is downwards; otherwise, it is upwards. Since the curve of interest has upward concavity, Eq. (23) is used. For ϕ = 0, t Eq. (23) reduces to Eq. (26).

$$z' = \frac{(H_0 - z) - R}{(X - x)} \quad \text{(eq. 26)}$$

The relationship between x and X is obtained through the energy balance method. When ϕ is equal to zero, the rays hitting the reflector at the point $x = x_{max}$ are directed to P2 =(L, H_0), shown in Fig. 4, while the rays hitting the point $x = L$ are directed to the point P1 =$(-L, H_0)$. Through the energy balance method (Burkhard and Shealy, 1975), gives Eq. (27).

$$\tau \int_L^x dx = E \int_{-L}^X dX \quad \text{(eq. 27)}$$

where τ is the irradiance on the reflector and E is the irradiance on the receiver, both constant. Developing the integrals of Eq. (27), Eq. (28) is obtained.

$$X = \frac{\tau}{E}(x - L) - L \quad \text{(eq. 28)}$$

where

$$\frac{\tau}{E} = \frac{1}{C_f} \quad \text{(eq. 29)}$$

C_f is the flux concentration, the ratio between the irradiance on the receiver and the irradiance on the reflector. For ϕ = 0, a C_f is given by Eq. (30).

$$C_f = \frac{(C-1)}{2} \quad \text{(eq. 30)}$$

The region of the curve between the points x = 0 e x = L is constructed iteratively with Euler's method, such that the rays hitting a certain point with coordinates (x, z) in this region of the reflector are reflected to point P1. For this purpose, Eq. (23) is used, with the value of ϕ seen in Eq. (31).

$$\phi = arctan\left(\frac{L - x}{H_0 - z}\right) \quad \text{(eq. 31)}$$

The result of dividing the CPC curve into mirror segments to transform it into a Fresnel is illustrated in Fig. 5.

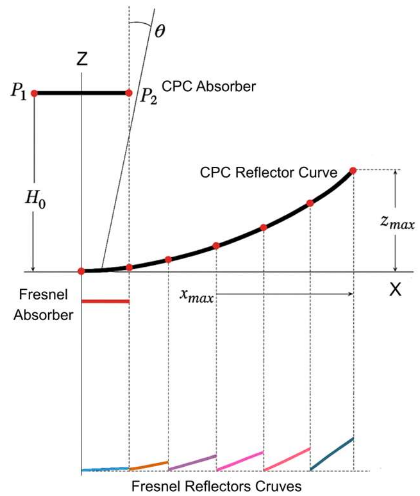

Figure 5. Geometry of the CPC changed to a Fresnel Linear.

In the development of the optimization, the first step is the Generation of the Ideal CPC Profile (Base Curve) using the Edge Ray Principle. For this, it uses the absorber half-width (L_{cpc}) the height ratio that defines the initial height ($H_{0,cpc}$), and implicitly the acceptance angle (θ_a). The profile is generated in two interconnected sections. The Direct Reflection Profile, generated numerically in an iterative way, ensuring that the rays starting from the absorber edge are directed to the exit aperture, and the Parabolic Segment, defined so that the incident rays at the maximum angle θ_a, upon reflecting in this section, hit the opposite edge of the absorber. The result is a continuous profile (r_p, x_p) which, despite being optically ideal, has an excessive height ($H_{0,cpc}$), confirming the need for the Fresnel modification.

This base curve is then transformed into a Fresnel-type concentrator through Aperture Segmentation and Calculation of the Tilt Angle (μ). The maximum aperture (r_{phmax}) is divided into N_e segments of width L_e. The Fresnel model assumes that each segment must redirect light with the same efficiency it would if it belonged to the original CPC curve, but from a more compact vertical position. The code calculates the center r_{psi} of each segment along the aperture and, for each center (r_{psi}, x_{pi}), , Eq. (32) determines the Ray Angle (ψ)) that connects this center on the original curve to the center of the absorber ($0, H_{abs}$), and also r_{psi}> 0.

$$\psi = arctan\left(\frac{H_{abs}-x_{pi}}{0-r_{psi}}\right) \quad \text{(eq. 32)}$$

The Fresnel Mirror Tilt Angle (μ) is then determined from ψ , through a geometric relationship derived from the law of reflection, which ensures that the incident solar ray (assumed to be parallel to the Z-axis) is reflected towards the center of the absorber. This angle (μ) is the zenith angle by which each small mirror must be tilted to efficiently redirect the rays to the absorber.

$$\mu = \frac{\pi}{4} - \frac{\psi}{2} \quad \text{(eq. 33)}$$

The final stage is the Leveling and Alignment of Segments, manipulating the extracted segments to form the compact Fresnel profile. Each segment is extracted by interpolation from the original CPC curve, maintaining the original curved shape. Subsequently, the average vertical height of the centers of all segments is calculated. Finally, each segment is vertically displaced so that its center coincides with this average height.

5. Results

The optical simulations were conducted using the ray-tracing software SolTrace, developed by the National Renewable Energy Laboratory (NREL), complemented by a custom Python script to automate ray generation and tracking. The primary objective of this section is to present and discuss the behavior of the crucial optical parameters, the Interception Factor (γ), the Uniformity Coefficient (U), and the Acceptance Angle (θ_a) as a function of the variation in the Concentration (C) for the studied models, as detailed in the Methodology.

The analysis of the V-Trough type concentrator focused on varying C while restricting it to the range of 1.4 to 2.0. This limitation is justified by the classification of solar concentration systems. According to the literature (Gallagher, 2008), concentrators with C between 1.1 and 2.0 can be operated with a fixed collector, simplifying the system and reducing costs. The simulation results for the V-Trough, values are presented in Table 2, demonstrated a clear and expected trend: increasing C resulted in a significant decrease in $\gamma$and θ_a.

Table 2: Behavior of the V-Trough concentrator parameters as a function of the Concentration Ratio variation.

C	γ	U	θ_a
1,4	0,999613	0,100244	45,58
1,5	0,999478	0,0981444	41,81
1,6	0,998927	0,0422022	38,68
1,7	0,949236	0,0296629	36,03
1,8	0,896268	0,0309502	33,75
1,9	0,849699	0,0322671	31,76
2	0,806787	0,0336794	30,00

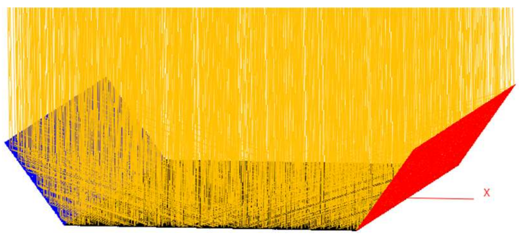

Figure 6. Model of the V-Trough concentrator on the SolTrace. Source: (Authors., 2025).

The original Truncated CPC, proposed by Xie et al. (2016), had a Concentration Ratio of C=4. The simulations explored both smaller and larger C values around this reference point. The most relevant result was obtained by reducing the Concentration Ratio to C =3.25. This modification resulted in superior performance across the three evaluated parameters: a high Interception Factor γ,approx 0.999), good uniformity (U 0.191), and, critically, an increase in the Acceptance Angle (θ_a = 14.03°) (Table 3).

Table 3: Behavior of the Truncated CPC parameters as a function of the Concentration variation.

C	γ	U	θ_a
3.25	0.99937	0.191011	14.03
3.5	0.999376	0.193947	12.71
4	0.999222	0.203169	10.6075
5	0.998942	0.20606	7.78187
6	0.998636	0.208996	5.9921
6.5	0.998356	0.211274	5.33

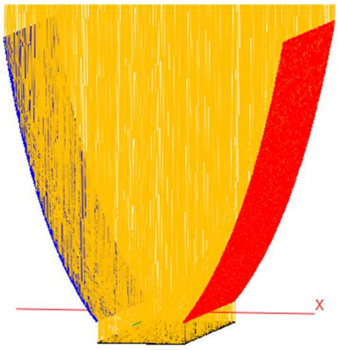

Figure 7. Model of the Truncated CPC on the SolTrace.

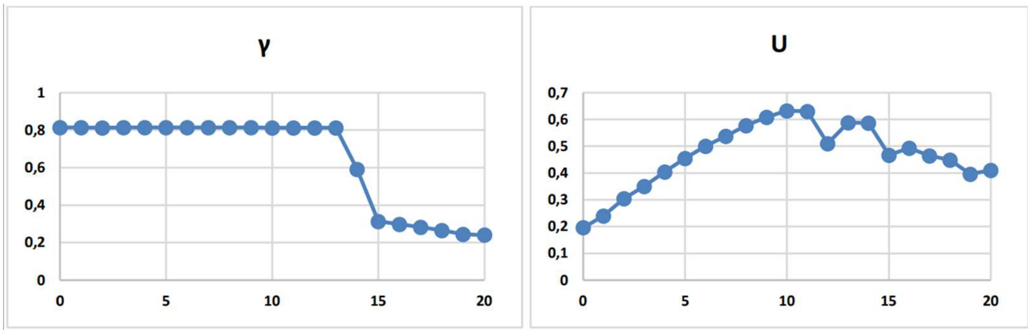

Figure 8. Curves of U and γ with valiation validating the θ_a.

Conversely, increasing C up to 6.5 showed the expected reduction in both γ e θ_a. However, U exhibited a slight increase. In CPC systems, concentration reduction (truncation) is often employed to lower the collector height, and in the case of C =3.25, the study demonstrated that this reduction was highly beneficial for the overall optical performance.

The CPC model developed in the present work achieved satisfactory values for γ = 0,969642 and U = 0,0891864. However, the resulting to θ_a was extremely low, close to 0.4°. To validate the simulation methodology and consistently determine o ângulo solar foi variado, para representar o seu movimento ao longo do dia e confirmar se o valor do γ iria reduzir quando o de θ_a fosse ultrapassado. O valor encontrado foi muito baixo, próximo de 0,4°.

To validate the simulation methodology and consistently determine θ_a, the collector testing criterion proposed by ASHRAE (2003) and discussed by Kalogirou (2014) was adapted. This criterion defines θ_a as the point at which the collector efficiency factor decays by no more than a predetermined percentage of its value at normal incidence.

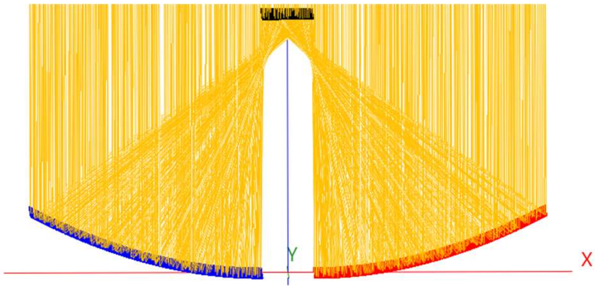

Figure 9. Model of the original CPC to be changed to a Fresnel on the SolTrace.

Given the strong influence of optical factors, the criterion was applied directly to γ, normalized relative to its maximum value (γ=0.970 at ϕ=0°). The analysis of the percentage drop in the Normalized Interception Factor as a function of the Solar Incidence Angle allowed for the determination of $\theta_a$under three distinct decay criteria:

- 1% decay: Determines the high-precision θ_a (applicable to sophisticated tracking systems).
- 2% decay: The adapted ASHRAE standard criterion (considered the reference).
- 5% decay: A more flexible criterion.

When comparing the results with the reference model (Kalogirou, 2014), the simulated behavior was found to follow the coherent trend that a greater angular deviation leads to a lower γ. However, the studied model showed superior performance in the initial operating range, maintaining interceptions above 0.9 even at more significant angular deviations than predicted by the literature for minimal solar error conditions.

In an attempt to maintain the CPC's optical performance, the geometry was transformed into a Fresnel concentrator. Although the geometric adjustments were theoretically coherent, the results of this conversion were unsatisfactory. The obtained γ was significantly low (close to 0.75 after adjustments to the concentration ratio), demonstrating a substantial optical loss compared to the original CPC. This outcome indicates that the geometric transformation, or the specific configuration of the Fresnel steps, failed to replicate the concentration and uniformity capability of the CPC.

6. Conclusion

This study performed a comparative and optimization analysis of optical parameters in non-imaging solar concentrators, utilizing ray-tracing simulation (SolTrace) and focusing on the variation of the Concentration Ratio (C).

Overall, the Optimized Truncated Compound Parabolic Concentrator (CPC) by Xie et al. (2016) proved to be the most promising model. By means of an adjustment in the Concentration Ratio (from C =4 to C =3.25), superior results were achieved in the critical optical performance parameters. Specifically: A concomitant improvement was observed in θ_a, γ and U The increase in θ_a to 14.03° is particularly relevant, as it significantly reduces the need for daily adjustments to the collector, simplifying operation and maximizing the capture of both diffuse and direct radiation throughout the day. The reduction in concentration implies a decrease in the concentrator's height, which is a positive factor for the constructability, material cost, and structural stability of the system.

The other geometry developed in the work (the proposed CPC) achieved good values for γ and U, but the extremely low θ_a (approx 0.4°) imposes a severe practical limitation, demanding ultra-high precision solar tracking and making it unviable for low-cost applications.

Finally, the transformation of the CPC into the Fresnel geometry did not yield satisfactory results, highlighting challenges in replicating the optical performance and maintaining a high γ.

7. References

Alami, A. H et al., 2023. Con-centrating solar power (CSP) technologies: Status and analysis. International Journal of Thermofluids. v. 18, 100340.

Burkhard, D. G., Shealy, D. L., 1975. Design of reflectors which will distribute sunlight in a specified manner. Solar Energy. 17, 221-227.

Chemisana, D., Ibáñez, M., Barrau, J., 2009. Comparison of Fresnel concentrators for building integrated photovoltaics. Energy Convers. Manag. 50, 4, 1079-1084.

Cuevas, A., López-Romero, S., 1984. The combined effect of non-uniform illumination and series resistance on the open-circuit voltage of solar cells. Physics, Engineering, Environmental Science Solar Cells. Published 1 March 1984.

Dhakal, R. et al., 2014. Bio-inspired thin and flat solar concentrator for efficient, wide acceptance angle light collection. Appl. Opt. 53, 2, 306-315.

Fraidenraich, N., Almeida, M. C., 1991. Optical properties of V-trough concentrators. Solar Energy. 47, 3, 147-155.

GALLAGHER, J. J., 2008. Nonimaging optics in solar energy. Morgan & Claypool.

GARLET, T. B. et al., 2020. Value chain in distributed generation of photovoltaic energy and factors for competitiveness: A systematic review. Solar Energy. 211, 396-411.

HASAN, H. A. et al., 2024. Experimental evaluation of thermal efficiency, electrical efficiency, and power production of low-concentrating photovoltaic-thermal system with micro-jet channel. Applied Thermal Engineering. 236.

INDIRA, S. S. et al., 2021. Optical performance of a hybrid compound parabolic concentrator and parabolic trough concentrator system for dual concentration. Sustainable Energy Technologies and Assessments. 47, 101538.

KALOGIROU, S. A., 2014. Solar Energy Engineering: Processes and Systems, 2nd ed. Elsevier, Estados Unidos.

KOLAMROUDI, M. K. et al., 2023. A comparative study of LCPV by mirror reflection against other systems: Recent techniques, implications, and performances. Solar Energy. 250, 70-90.

LOFTI, M. et al., 2022. Experimental study on simultaneous use of phase change material and reflector to enhance the performance of photovoltaic modules. Journal of Energy Storage. 54.

PARUPUDI, R. V. et al., 2020. Low Concentrating Photovoltaics (LCPV) for buildings and their performance analyses. Applied Energy. 279, 115839.

PRASAD, G. S. et al., 2017. Optimization of solar linear Fresnel reflector system with secondary concentrator for uniform flux distribution over absorber tube. Solar Energy. 150, 1-12.

Regany et al., 2025. Enhancing efficiency of dense array CPV receivers with controlled DC-DC converters and adaptive microfluidic cooling under non-uniform solar irradiance. Solar Energy Materials and Solar Cells. 279, 19.

SOUZA, L. F. L., 2022. Concentrador Linear Fresnel aplanático. Tese (Doutorado em Tecnologias Energéticas e Nucleares). Universidade Federal de Pernambuco, Departamento de Energia Nuclear, Recife.

USTAOGLU, A. et al., 2023. Performance investigation of truncated low concentrating photovoltaic-thermal systems with V-trough, compound hyperbolic and compound parabolic concentrators. Applied Thermal Engineering. 232, 121028.

WANG et al., 2020. Design and thermodynamic analysis of a novel solar CPV and thermal combined system utilizing spectral beam splitter. Renewable Energy. 155, 1091-1102.

XIE, H. et al., 2016. Design and performance study of truncated CPC by eliminating multiple reflections of solar radiation in hybrid CPV/T system: Highest and lowest truncation position. Solar Energy. 136.